

# Maximizing the response of SPR signal: A vital role of light excitation wavelength

Cite as: AIP Conference Proceedings **2016**, 020104 (2018); <https://doi.org/10.1063/1.5055506>  
Published Online: 27 September 2018

Wan Maisarah Mukhtar, Noor Faezah Murat, Nurul Diyanah Samsuri, and Karsono Ahmad Dasuki



View Online



Export Citation

## ARTICLES YOU MAY BE INTERESTED IN

[Study on plasmon absorption of hybrid Au-GO-GNP films for SPR sensing application](#)  
AIP Conference Proceedings **1972**, 030007 (2018); <https://doi.org/10.1063/1.5041228>

[Influence of annealing temperature on optical properties of Al doped ZnO nanoparticles via sol-gel methods](#)

AIP Conference Proceedings **1972**, 030006 (2018); <https://doi.org/10.1063/1.5041227>

[Preface: The 3rd International Conference on Applied Science and Technology \(ICAST'18\)](#)  
AIP Conference Proceedings **2016**, 010001 (2018); <https://doi.org/10.1063/1.5055402>

Lock-in Amplifiers

Zurich Instruments

Watch the Video

# Maximizing the Response of SPR Signal: A Vital Role of Light Excitation Wavelength

Wan Maisarah Mukhtar<sup>1,a)</sup>, Noor Faezah Murat<sup>1,b)</sup>, Nurul Diyanah Samsuri<sup>1,c)</sup> and Karsono Ahmad Dasuki<sup>1,d)</sup>

<sup>1</sup>Faculty of Science and Technology, Universiti Sains Islam Malaysia (USIM), Bandar Baru Nilai, 71800 Nilai, Negeri Sembilan, Malaysia.

<sup>a)</sup>Corresponding author: [wmaisarah@usim.edu.my](mailto:wmaisarah@usim.edu.my)

<sup>b)</sup>[fzhmrt@raudah.usim.edu.my](mailto:fzhmrt@raudah.usim.edu.my)

<sup>c)</sup>[diyanah.fst@gmail.com](mailto:diyanah.fst@gmail.com)

<sup>d)</sup>[drkarsono@usim.edu.my](mailto:drkarsono@usim.edu.my)

**Abstract.** Criteria for development of high sensitivity surface plasmon resonance (SPR) sensor depends on several factors such as types of metals, light polarization modes, light coupling techniques and thicknesses of metal film. This paper discussed the effect of light excitation wavelength ranging from ultra violet (UV) region to infrared (IR) region on SPR. Three regions have been classified such as UV region (from  $\lambda=200\text{nm}$  to  $\lambda=380\text{nm}$ ), visible region (from  $\lambda=400\text{nm}$  to  $\lambda=633\text{nm}$ ) and IR region (from  $\lambda=870\text{nm}$  to  $\lambda=1550\text{nm}$ ). Noble metal gold thin film with thickness of 50nm and refractive index of  $n=0.1759+3.3104k$  was deposited on top of BK7 triangular prism ( $n=1.51$ ). Very weak SPR signal was generated as the excitation wavelength was set in UV region. The signal's strength increased about 26.63% with the increment of wavelength from  $\lambda=200\text{nm}$  until  $\lambda=380\text{nm}$ , resulting the blue-shifting of SPR angle from  $54.03^\circ$  to  $43.48^\circ$ . The greatest excitation of SPP was significantly observed as the visible light region was incident through the thin film gold-coated prism represented by the abrupt decreased of  $R_{\min}$  to 96.50% at  $\lambda=633\text{nm}$ . The SPR angle was red-shifted about  $0.30^\circ$  throughout this region. The SPR signal getting weaker as light excitation wavelength entered the IR region (from  $\lambda=870\text{nm}$  to  $\lambda=1550\text{nm}$ ) indicated by the 64.34% inclination of  $R_{\min}$ . In this region, the SPR angle was remain red-shifted from  $\theta_{\text{SPR}}=44.97^\circ$  until  $\theta_{\text{SPR}}=46.18^\circ$  with the average increment of  $0.31^\circ$  for each wavelength. It can be concluded that the usage of red laser,  $\lambda=633\text{nm}$  able to enhance the maximum excitation of SPP. The remarkable outcome of this work shows the vital role of light excitation wavelength in generating strong SPR signal for various application such as sensor and optoelectronic device.

## INTRODUCTION

Until today, public awareness on environmental pollution is still at low level [1, 2]. The dangers of environmental pollution such as water pollution have negatively affected lives such as death and disability. The disposal of waste product to the environment from industry leads to the pollution and health issues. Water sources such as river and sea are the most common media which able to spread hazardous chemical such as lead (Pb), mercury (Hg) and other heavy metal ions. Exposure to heavy metal ions may interfere the brain development and the nervous system and cause the high blood pressure and kidney damage [3]. Today, development of several types of sensors such as mechanical sensor [4, 5], electrochemical sensor [6, 7] and optical sensor [8, 9] become one of the precaution alternative towards the health society.

Optical sensor is one of the favorable sensor due to its high sensitivity in detecting the presence of heavy metal ions [10]. Optical sensor can be divided into two, which are fiber optics sensor and free-space sensor. The main principle of fiber optics sensor is the used optical fiber as the vital sensing medium. By manipulating the properties of

optical fiber itself such as decreasing thickness of cladding [11-13], manipulating the bending losses [14-16] and appointment of thin film and nanoparticles [17, 18] on the cladding surface, the fiber optics sensor able to be developed. However, the main challenges in developing this type of sensor is due to its expensive and complicated fabrication procedure. Free-space sensor is more convenient by considering its reliability, high sensitivity and simple fabrication steps. Surface plasmon resonance (SPR) sensor is a famous optical sensor due to its versatility and less-complicated working principle. Its working principle depends on the change of refractive index (RI) of the sensing medium as reported elsewhere [19,20].

Main requirements for the development of SPR sensor are metal thin film with thickness less than 100nm, prism for light coupling and the appointment of p-polarized laser source [21,22]. Selection of suitable thicknesses mainly affect the sensitivity of SPR sensor, too thick thin film which is more 100nm results the absence of evanescent field due to the light absorbance inside metal thick film. Meanwhile, a very thin film which is less than 30nm may leads to electron damping oscillations [23]. Shape of prism also influence the amount of incident light to be coupled at metal-air boundary. Half-cylindrical and triangular prism able to produce maximum light coupling as discussed in our previous work [24]. The usage of p-polarized results the optimization of SPR signal up to 50% in comparison with the circular-polarized light. Note that the appointment of p-polarized light is also depends on the light wavelength. Usually, helium neon red laser ( $\lambda=633\text{nm}$ ) is commonly used due to its better visibility and able to provide a Gaussian beam shape with low divergence [25-27]. Nonetheless, type of laser for the generation of SPR is not only limited to this respective wavelength as there are few SPR works employing another wavelength source yet resulting good SPR signal [28].

This paper discussed the potential of electromagnetic waves ranging from ultra violet (UV) region to infrared (IR) region to excite surface plasmon polaritons (SPP). Gold thin film with thickness of 50nm remain fixed throughout this work. The significant output of this research exhibits the versatility of SPR signal's strength as the value of excitation wavelength is modulated.

## METHODOLOGY

Gold thin film (refractive index,  $n=0.1758+3.4101k$ ) with thickness of 50nm was deposited on top the hypotenuse side of a BK7 glass prism ( $n=1.51$ ) using Kretschmann configuration. The main function of prism was to couple the incident light so that sufficient energy able to excite surface plasmon polaritons (SPP). p-polarized light source was incident through the gold-coated prism for the generation of SPR signal as illustrated in Fig. 1.

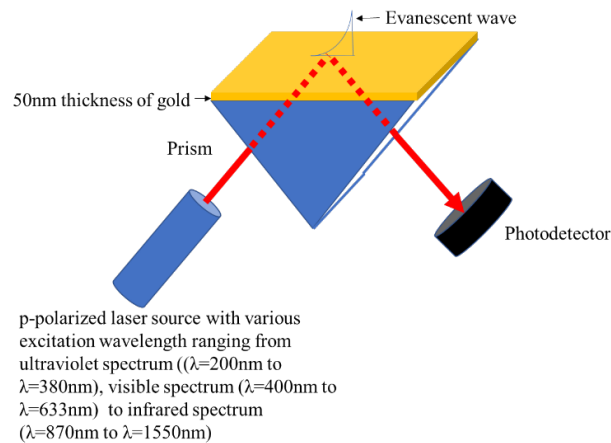


**FIGURE 1.** Proposed SPR experimental setup which consisted of p-polarized light source with various excitation wavelength, prism which acted a light coupler and gold thin film to generate the surface plasmon polaritons (SPP)

In this work, three regions of light spectra with various wavelength were employed such as ultraviolet spectrum ( $\lambda=200\text{nm}$  until  $\lambda=380\text{nm}$ ), visible spectrum ( $\lambda=400\text{nm}$  until  $\lambda=633\text{nm}$ ) and infrared spectrum ( $\lambda=870\text{nm}$  until  $\lambda=1550\text{nm}$ ) by using an angular interrogation technique. The characterization of SPR signal for each wavelength was investigated by studying the important parameters on SPR curves such as minimum reflectance ( $R_{\min}$ ), SPR angle and amount of angle shifting. The smaller the minimum reflectance, the greater the amount of SPP's excitation due to the large part of incident light which was successfully absorbed by the gold thin films resulting the presence of evanescent field [29].

## RESULTS & DISCUSSIONS

Figure 2 illustrates the SPR curves for various light excitation wavelength. The employment of light source with excitation wavelength in UV spectrum range resulted weak SPR signals as shown in Fig. 3(a). At  $\lambda=200\text{nm}$ , no SPR signal was observed. As value of wavelength was increased to  $\lambda=250\text{nm}$ , a very shallow SPR peak with minimum reflectance,  $R_{\min}=0.8181$  a.u was obtained indicated the existence of weak evanescent field due to the excitation of SPP.  $R_{\min}$  was decreased about 4.89% with the recorded value of  $R_{\min}=0.7780$  a.u as the excitation wavelength was tuned to  $\lambda=300\text{nm}$ . Similar patterns were observed where the value of  $R_{\min}$  became smaller with the increment of excitation wavelength from  $\lambda=320\text{nm}$  until  $\lambda=380\text{nm}$ . The lowest value of  $R_{\min}=0.6063$  a.u was achieved at  $\lambda=380\text{nm}$  proving that the strongest SPR signal able to be generated in UV region by employing this respective wavelength. A significant output was resulted as the spectrum region changed from UV to the visible as depicted in Fig. 3(b). Strong SPR was generated when the wavelength was set at  $\lambda=633\text{nm}$  (red colour laser) where the smallest value of  $R_{\min}=0.014$  a.u obtained. We observed weak SPR signal at  $\lambda=400\text{nm}$  which was very near to the boundary between UV region and visible region. Yet, with the increment of wavelength from blue-violet light ( $\lambda=400\text{nm}$ ) to red light ( $\lambda=633\text{nm}$ ),

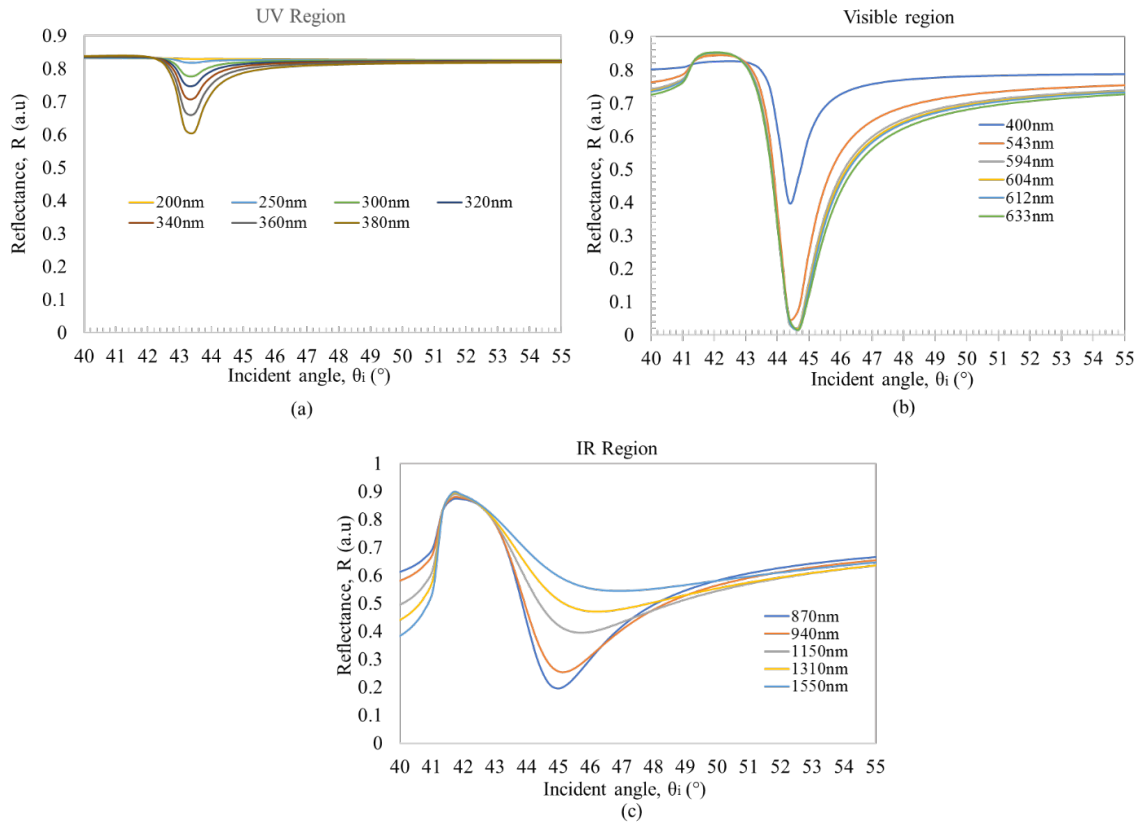


**FIGURE 2.** SPR curves as p-polarized light with various wavelengths were incident through the 50nm thickness of gold-coated triangular prism (a) ultra violet region ( $\lambda=200\text{nm}$  until  $380\text{nm}$ ) (b) visible region ( $\lambda=400\text{nm}$  until  $\lambda=633\text{nm}$ ) (c) infrared region ( $\lambda=870\text{nm}$  until  $1550\text{nm}$ )

the SPR phenomena became more significant. Starting from  $\lambda=543\text{nm}$  (green light), value of  $R_{\min}$  dropped about 87.44% to 0.0502 a.u in comparison with reflectance value at  $\lambda=400\text{nm}$ . At  $\lambda=604\text{nm}$ ,  $R_{\min}$  was obtained as 0.019 a.u. Value of  $R_{\min}$  was slightly reduced to  $R_{\min}=0.016$  a.u and  $R_{\min}=0.014$  a.u as the wavelengths were set at  $\lambda=612\text{nm}$  and  $\lambda=633\text{nm}$ , respectively. This impressive output indicated the vital role of excitation wavelength as a control parameter in creating strong SPR. Value of  $R_{\min}$  started to increase about 92.83% as the excitation wavelength was shifted to IR region light source at  $\lambda=870\text{nm}$  as indicated in Fig. 3(c). As the light's wavelength fixed at  $\lambda=940\text{nm}$ , value of  $R_{\min}$  was recorded as 0.2561 a.u. This increment pattern had been observed throughout this region where the largest  $R_{\min}$  was achieved at  $\lambda=1550\text{nm}$  with  $R_{\min}=0.5477$  a.u.

Apart from the value of minimum reflectance, the sensitivity of SPR sensor was commonly observed based on the amount of angle shifting. Fig. 4 exhibits the response of  $R_{\min}$  and SPR angle as the excitation wavelengths were varied. Value of  $R_{\min}$  decreased to 26.63% with the increment of the wavelength in UV region from  $\lambda=200\text{nm}$  until  $\lambda=380\text{nm}$  (Fig. 3(a)). The SPR angle was blue-shifted from  $54.03^\circ$  to  $43.48^\circ$  as the wavelength was tuned from  $\lambda=200\text{nm}$  to  $\lambda=250\text{nm}$ . No notable change on SPR angle was observed when the value of wavelength was modulated from  $\lambda=250\text{nm}$  until  $\lambda=380\text{nm}$  where the angle remained at  $\theta_{\text{SPR}}=43.48^\circ$ . An abrupt declination of  $R_{\min}$  was resulted in visible region when it approached  $\lambda=543\text{nm}$  as illustrated in Fig. 3(b).  $R_{\min}$  reached its minimum value at  $\lambda=633\text{nm}$  with percentage of drop about 96.50% in comparison with blue-violet wavelength ( $\lambda=400\text{nm}$ ). The SPR angles remained constant at  $\theta_{\text{SPR}}=44.37^\circ$  with the increment of wavelength from  $\lambda=400\text{nm}$  to  $\lambda=543\text{nm}$ . The SPR angle was then red-shifted at  $\lambda=594\text{nm}$  with  $\theta_{\text{SPR}}=44.67^\circ$  and consistent at this angle until  $\lambda=633\text{nm}$ . Value of  $R_{\min}$  was linearly increased up to 64.34%, from  $R_{\min}=0.1953$  a.u ( $\lambda=870\text{nm}$ ) to  $R_{\min}=0.5477$  a.u ( $\lambda=1550\text{nm}$ ) as its entered the IR region (Fig. 3(c)). The shifting of SPR angle portrayed the same behavior as in the visible region, where the red-shifted of angle was resulted. Interestingly, the SPR angle consistently red-shifted from  $\theta_{\text{SPR}}=44.97^\circ$  until  $\theta_{\text{SPR}}=46.18^\circ$  with the average increment of  $0.31^\circ$  for each wavelength.

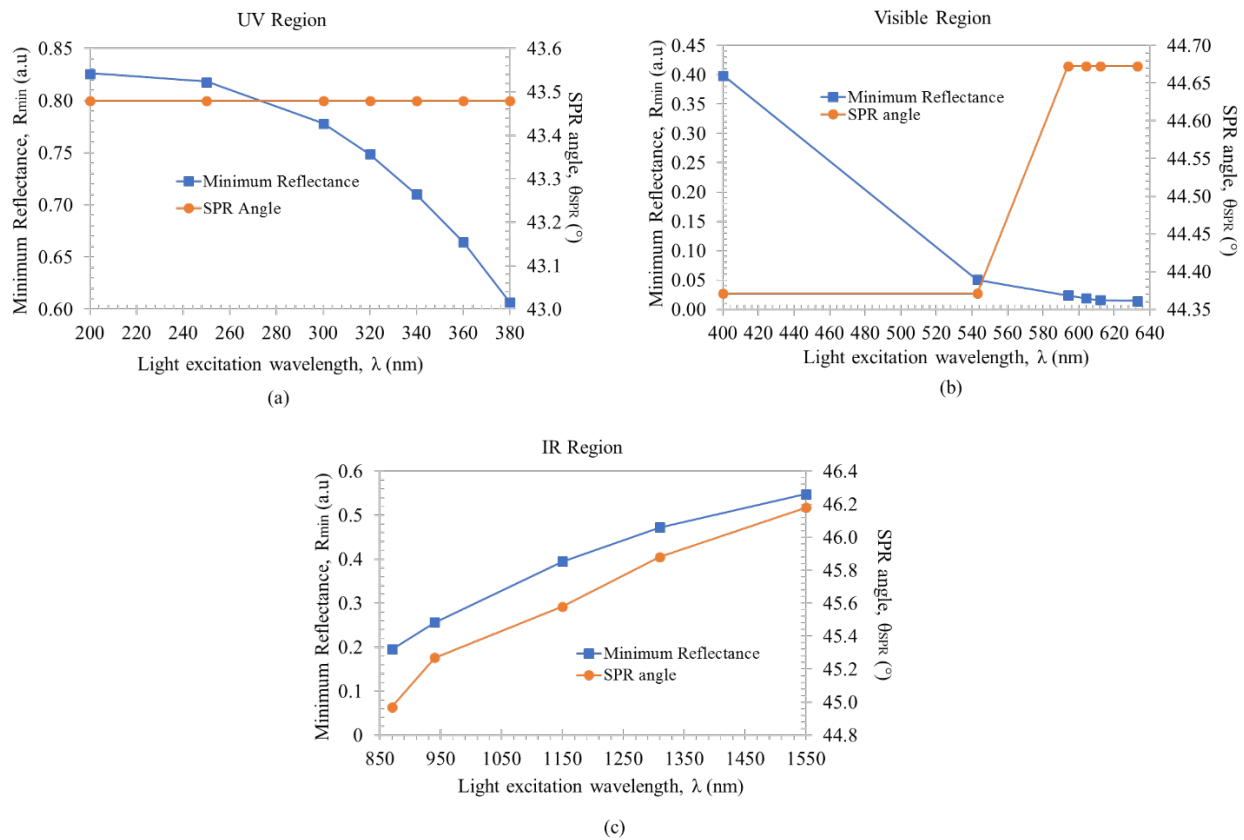


**FIGURE 3.** Response of  $R_{\min}$  and SPR angle as the excitation wavelengths were varied. (a) ultra violet region ( $\lambda=200\text{nm}$  until  $380\text{nm}$ ) (b) visible region ( $\lambda=400\text{nm}$  until  $\lambda=633\text{nm}$ ) (c) infrared region ( $\lambda=870\text{nm}$  until  $1550\text{nm}$ )

Figure 4 shows the effect of each region on the value of  $R_{\min}$  and SPR angle as the excitation wavelength increased. Combination features of unshifted SPR angle and large value of  $R_{\min}$  in UV region indicates the unsuitability of this region to be employed as light source to generate SPR signal. As the wavelengths were tuned into visible region, the  $R_{\min}$  was significantly decreased which exhibits a high potential candidate for the development of excellent sensitivity SPR sensor. The SPR signal became stronger as the value of excitation wavelength increased from UV region to visible region. The strongest signal was obtained at  $\lambda=633\text{nm}$  validating the eligibility of this wavelength to excite maximum excitation of SPP. This is due to the strong coupling between light and surface charges where the light field has to drag the electrons along the metal surface. The SPP on a plane interface cannot be excited by light of any frequency that propagates in free space [23]. SPR angles were red-shifted about 0.68% from  $44.731^\circ$  to  $44.673^\circ$  as the wavelength were modulated between  $\lambda=400\text{nm}$  and  $\lambda=633\text{nm}$ . As excitation wavelength entered the IR region, value of  $R_{\min}$  was abruptly inclined indicated a low excitation of SPP. The SPR angle experienced red-shifting throughout this region.

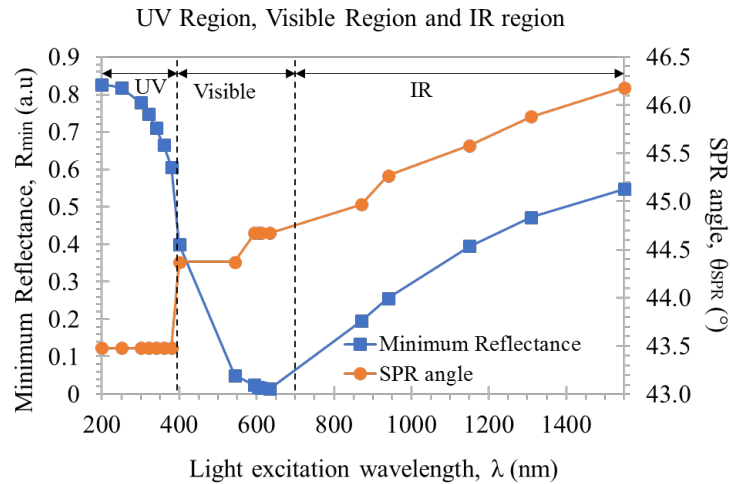


**FIGURE 4.** Effect of light excitation wavelength on the value of minimum reflectance,  $R_{\min}$  and location of SPR angle,  $\theta_{\text{SPR}}$ . Strong SPR signal was obtained in visible region.

## CONCLUSION

Recently, SPR sensor has been actively developed for numerous applications due to its high sensitivity and simplicity. In this work, we were successfully enhanced the SPR signal's strength by manipulating the value of light excitation wavelength from UV region to IR region. The employment of visible light at  $\lambda=633\text{nm}$  exhibits maximum generation of SPP. We believe that this discovery will benefits to the development SPR sensor with impressive versatility.

## ACKNOWLEDGEMENTS

The authors would like to acknowledge the support of the Universiti Sains Islam Malaysia (USIM) and Kementerian Pengajian Tinggi Malaysia (KPT) for funding this work under grant USIM/FRGS/FST/32/51514. Knoll Group from Max Planck Institute for Polymer Research, German is also acknowledged for the Winspall 3.02 simulation software.

## REFERENCES

1. M. G. Wani, Bull. Env. Pharmacol. Life Sci **3**, 10-12 (2014).
2. F.J. Kelly & J. C. Fussell, *Environmental Geochemistry and Health*, **37**, 631-649 (2015).

3. D. Lakherwal, International Journal of Environmental Research and Development, **4**, 41-48 (2014).
4. L. Lin, S.Wang, S. Niu, C. Liu, Y. Xie, Y and Z. L. Wang, *ACS Applied Materials & Interfaces*, **6**, 3031-3038 (2014).
5. O. Alvear, W. Zamora, C. T. Calafate, J. C. Cano and P. Manzoni, "EcoSensor: Monitoring environmental pollution using mobile sensors" in *World of Wireless, Mobile and Multimedia Networks (WoWMoM), 2016 IEEE 17th International Symposium on A* (IEEE, 2016), pp. 1-6.
6. N. Ruecha, N. Rodthongkum, D. M. Cate, J. Volckens, O. Chailapakul and C. S. Henry, *Analytica Chimica Acta*, **874**, 40-48 (2015).
7. Y. Zhang, G. M. Zeng, L. Tang, J. Chen, Y. Zhu, X. X. He and Y. He, *Analytical Chemistry*, **87**, 989-996 (2015).
8. F. Starecki, F. Charpentier, J.L. Doualan, L. Quetel, K. Michel, R. Chahal, J. Troles, B. Bureau, A. Braud, P. Camy, V. Moizan, and V. Nazabal, *Sensors and Actuators B: Chemical*, **207**, 518-525 (2015).
9. K. Murphy, B. Heery, T. Sullivan, D. Zhang, L. Paludetti, K. T. Lau, D. Dermot, C. Ernane, O. C. and F. Regan, *Talanta*, **132**, 520-527 (2015).
10. W. M. Mukhtar, R. M. Halim, K.A Dasuki, A.R.A. Rashid and N.A.M Taib, *Malaysian Journal of Fundamental and Applied Sciences* **13**, (2017).
11. W. M. Mukhtar, S. Shaari and P. S. Menon, "Fabrication of optical fiber microprobe using electric arc heating and one-sided pulling technique" in *Research and Development (SCORED), 2010 IEEE Student Conference on* (IEEE, 2010), pp. 104-106.
12. W. M. Mukhtar, P. S. Menon, P. S. and S. Shaari, S. "Effect of taper angle of the optical fiber microprobe in power collection" in *Advanced Materials Research* (Trans Tech Publications, 2012), pp. 3387-3391.
13. A. R. A. Rashid, A. A. Nasution, A. H. Suranin, N. A. Taib, W. M. Mukhtar, K. A. Dasuki, K. A. and A. A. Ehsan, "Chemical tapering of polymer optical fiber" in *InCAPE2017 EPJ Web of Conferences* **162**, edited by M. H. A. Wahid (EDP Sciences, France, 2017), pp. 01015.
14. T. Von Lerber and M. W. Sigrist, *Applied Optics*, **41**, 3567-3575 (2002).
15. W. Li, S. C. M., Ho, M. Luo, Q. Huynh and G. Song, *Smart Materials and Structures*, **26**, 045002 (2017).
16. W. M. Mukhtar, N. A. Marzuki and A. R. A. Rashid, *Journal of Advanced Research in Applied Sciences and Engineering Technology*, **9**, 14-21 (2017).
17. G. M. Shukla, T. Kundu, T. and S. Mukherji, "Decahedral Silver Nanoparticles Coated U-Shaped Fiber Optic Sensor for Mercury Detection" in *International Conference on Fibre Optics and Photonics* (Optical Society of America, 2016), pp. 65.
18. N. D. Samsuri, W. M. Mukhtar, A. R. A. Rashid, K. A. Dasuki and A. A. R. A. Yussuf, "Synthesis methods of gold nanoparticles for Localized Surface Plasmon Resonance (LSPR) sensor applications" in *InCAPE2017 EPJ Web of Conferences* **162**, edited by M. H. A. Wahid (EDP Sciences, France, 2017), pp. 01002.
19. M. Y. Pan, K. L. Lee, L. Wang and P. K. Wei, *Biosensors and Bioelectronics*, **91**, 580-587 (2017).
20. C. L. Wong and M. Olivo, *Plasmonics*, **9**, 809-824 (2014).
21. N. F. Murat, W. M. Mukhtar, A. R. A. Rashid, K. A. Dasuki and A. A. R. A. Yussuf, "Optimization of gold thin films thicknesses in enhancing SPR response" in *Semiconductor Electronics (ICSE), 2016 IEEE International Conference on* (IEEE, 2016), pp. 244-247.
22. N. F. Murat, W. M. Mukhtar, P. S. Menon, A. R. A. Rashid, K. A. Dasuki and A. A. R. A. Yussuf, "Influence of electromagnetic (EM) waves polarization modes on surface plasmon resonance" in *InCAPE2017 EPJ Web of Conferences* **162**, edited by M. H. A. Wahid (EDP Sciences, France, 2017), pp. 01008.
23. L. Novotny and B. Hecht, *Principles of Nano-optics*. (Cambridge University Press, United Kingdom, 2012), pp. 387-392.
24. W. M. Mukhtar, R. M. Halim and H. Hassan, "Optimization of SPR signals: Monitoring the physical structures and refractive indices of prisms," in *InCAPE2017 EPJ Web of Conferences* **162**, edited by M. H. A. Wahid (EDP Sciences, France, 2017), pp. 01001.
25. G. R. Hanes, K. M. Baird and J. DeRemigis, *Applied optics*, **12**(7), 1600-1605 (1973).
26. L. Pei, Y. Ou, W. Yu, Y. Fan, Y. Huang, Y. and K. Lai, *Journal of Nanomaterials*, **16**(1), 215 (2015).
27. Jiang, J., Xu, Z., Ameen, A., Ding, F., Lin, G., & Liu, G. L. *Nanotechnology*, **27**(38), 385205 (2016).
28. N. Hidaka, Y. Kuroda, Y. Matsushima and K. Utaka, "Polymer waveguide-type Kretschmann-structure surface plasmon sensor at 1550nm wavelength range" in *Microoptics Conference (MOC) 2013 18<sup>th</sup>*, (IEEE, 2013), pp. 1-2.
29. W. M. Mukhtar, S. Shaari, A. A. Ehsan and P. S. Menon, *Optical Materials Express*, **4**, 424-433 (2014).